Large density variation predicted along the magnetic axis for cold electron plasmas in the Columbia Nonneutral Torus (CNT)

Remi G. Lefrancois and Thomas Sunn Pedersen
Department of Applied Physics and Applied Mathematics, Columbia University, New York, New York 10027

(Received 2 October 2006; accepted 13 November 2006; published online 13 December 2006)

Cold pure electron plasmas confined in Penning-Malmberg traps with mirror fields are known to exhibit density variations along field lines, such that the density is roughly proportional to the magnetic field strength, $n \sim B$. The Columbia Nonneutral Torus (CNT) is the first stellarator designed to study pure electron plasmas, and exhibits substantial mirroring, with $B_{\max} \approx 1.8 B_{\min}$. However, results of a three-dimensional equilibrium solver, presented in this Letter, predict a factor of 5.3 increase in density from the minimum-field cross section to the maximum-field cross section along the magnetic axis, for a 1.5 cm Debye length plasma ($a \approx 15$ cm for CNT). In this Letter, it is shown that the density variation of electron plasmas in mirror traps can be significantly enhanced in a device that has a cross section that varies from cylinder-like to slab-like, such as the CNT. A simple analytic expression is derived that describes the axial density variation in such a device, and it is found to agree well with the computational predictions for CNT. © *2006 American Institute of Physics*. [DOI: 10.1063/1.2405341]

The study of non-neutral plasmas confined in stellarators has only recently begun, and is currently being pursued experimentally and theoretically by the Columbia Nonneutral Torus (CNT) group.[1] An understanding of the confinement of non-neutral plasmas on magnetic surfaces is not only of interest from a basic plasma physics point of view, but may also yield insights of importance to traditional fusion research. This type of confinement scheme allows us to investigate transport through the full range of charge imbalance, from the "extreme" ion root ($e\phi \gg T_e$) to quasi-neutrality. Furthermore, excellent predicted particle confinement times for a high charge imbalance [$\tau_p \sim (e\phi/T_e)^2 \tau_e \gg \tau_e$, where τ_e is the electron collision time] suggest that this type of confinement may be a candidate for the production of a neutral antihydrogen—a possible alternative to Penning traps.[2]

The equilibrium exhibited by such a plasma is fundamentally different from the equilibrium of quasi-neutral plasmas: non-neutrality means that the electrostatic term cannot be dropped from the fluid force balance, and low density results in the magnetic field being independent of the plasma current.[3] In this Letter we focus on one particular aspect of the equilibrium of such plasmas—the variation of density along the magnetic axis. This potentially large variation in density along the magnetic field is an effect that is not present for quasi-neutral plasmas in tokamaks or stellarators. It is, however, exhibited by non-neutral plasmas in cylindrical mirror traps,[4] where the density is proportional to the magnetic field strength. This density variation is enhanced by the highly shaped magnetic surface configuration of CNT—a factor of 5.3 density variation is predicted along the magnetic axis, whereas the magnetic field strength only varies by a factor of 1.8. In this Letter, computational results from a full three-dimensional (3D) equilibrium solver are presented for the toroidal density variation in CNT, and a simple relation is derived to reconcile these results with those reported for cylindrical mirror traps.[4]

The fluid force balance equation for a low density [$n_e \ll n_B = \epsilon_0 B^2/2m_e$ (Ref. 5)] pure electron plasma is given by 3

$$0 = -en_e(\vec{E} + \vec{u_e} \times \vec{B}) - \vec{\nabla} P. \tag{1}$$

Taking the dot product of Eq. (1) with $\vec{B}$, the parallel force balance is obtained:

$$en_e \frac{\partial \Phi}{\partial \ell} = T_e(\psi) \frac{\partial n_e}{\partial \ell}, \tag{2}$$

where ℓ is a spatial coordinate along the magnetic field and Ψ is the magnetic flux coordinate. Noting that $e\Phi/T_e \approx (a/\lambda_d)^2$ for a single-species plasma, where $\lambda_D = \sqrt{\epsilon_0 T_e/e^2 n_e}$ is the Debye length, a crude relation between relative variations in density and potential along a field line is obtained:

$$\frac{\Delta n_e}{n_e} \approx \frac{e\Delta\Phi}{T_e} \approx \left(\frac{a}{\lambda_D}\right)^2 \frac{\Delta\Phi}{\Phi}. \tag{3}$$

Equation (3) illustrates a key feature of pure electron plasmas confined on magnetic surfaces: density and potential are not in general constant along field lines in these plasmas, and the relative variations of the two are related by the number of Debye lengths in the plasma. In the hot limit ($a/\lambda_D \to 0$), the electron density becomes constant along the field, and in the cold limit ($a/\lambda_D \to \infty$), the plasma potential is constant along field lines.

The fundamental equilibrium equation is obtained from Eq. (2) by integrating along the field, solving for density, and combining with Poisson's equation[3]

$$\nabla^2 \Phi = \frac{e}{\epsilon_0} N(\psi) \exp\left(\frac{e\Phi}{T_e(\psi)}\right), \tag{4}$$

where $N(\Psi)$ is a sort of "weight function," having units of density, which describes the magnitude of the Boltzmann-

FIG. 1. (Color online) Cutaway view of the CNT magnetic surface configuration.

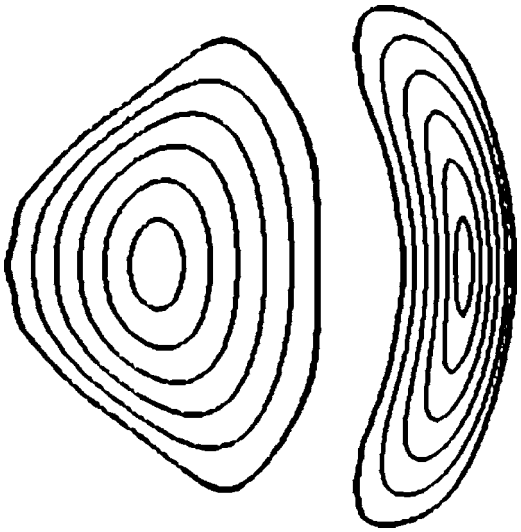

FIG. 3. (left) Cylinder-like CNT cross section at the minimum-field point. (right) Slab-like CNT cross section at the maximum-field point.

distributed density on each magnetic surface. Equilibrium solvers have been developed in two dimensions (2D)[6] and 3D[7]—in this Letter we use the 3D equilibrium solver to look at toroidal density variations along the magnetic field.

For a toroidally symmetric magnetic surface configuration, no toroidal variation of density along the magnetic axis will be observed. CNT, however, is far from toroidally symmetric, its cross section varying significantly in shape and size, as shown in Fig. 1.

A typical CNT plasma has a peak density on the order of 10^{12} m^{-3} and temperature around 5 eV, for a Debye length of around 1.5 cm. The minor radius of the device is roughly 15 cm, yielding an (a/λ_D) factor of about 10—a "cold" plasma. Figure 2 shows the computed normalized density

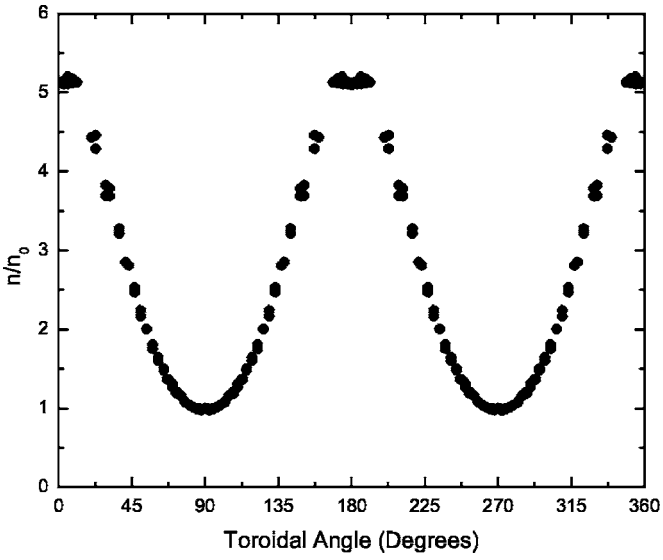

FIG. 2. Normalized axial density variation for a cold electron plasma, $a/\lambda_D \approx 10$.

along the magnetic axis for such a plasma, with a parabolic density profile enforced at the 0° cross section [this sets $N(\Psi)$ in Eq. (4)]. The equilibrium is solved on a 128^3 Cartesian grid, and density values are plotted for all points having $\Psi < 0.05\Psi_{\text{edge}}$.

A factor of 5.3 variation in density is predicted by the equilibrium solver, with the highest densities occurring at the smallest, highest-field, cross sections (90° and 270°) and the lowest densities at the largest, lowest-field, cross sections (0° and 180°). This is similar to the effect discussed by Fajans[4] for cylindrical mirror traps, in which the plasma density is proportional to the magnetic field strength. However, the magnetic field strength of the CNT varies only by a factor of 1.8 toroidally. This discrepancy is due to the unusual geometry of the CNT.

As shown by Fajans, for a Penning-Malmberg mirror trap having density $n=n_{\text{axis}}f(r)$, where n_{axis} is the density on axis and $f(r)$ is some function of radius,

$$\Delta\Phi \sim n_{\text{axis}}a^2 \sim \frac{n_{\text{axis}}}{B}. \tag{5}$$

Here, a is the variable radius of the confining region, and we have used the fact that $B \sim 1/a^2$. For a cold plasma, the voltage drop between the axis and the edge is a constant due to the constancy of potential along the field, and so from Eq. (5) we see that $n_{\text{axis}} \sim B$ for a Penning-Malmberg trap with varying magnetic field strength.

Although the cross section of the CNT is roughly circular at the low-field point, it is highly elongated at the high-field point, where the height of the cross section is roughly 4.5 times greater than the width (Fig. 3). By treating this cross section as a one-dimensional (1D) slab (infinite in extent in 2D) of half-width $w_{1/2}$, a proper estimate of the axial variation is obtained.

We consider plasmas with density of the form $n(q)=n_{\text{axis}}f(q)$, where q represents the radial and linear coordinates of the cylindrical and slab geometries, respectively.

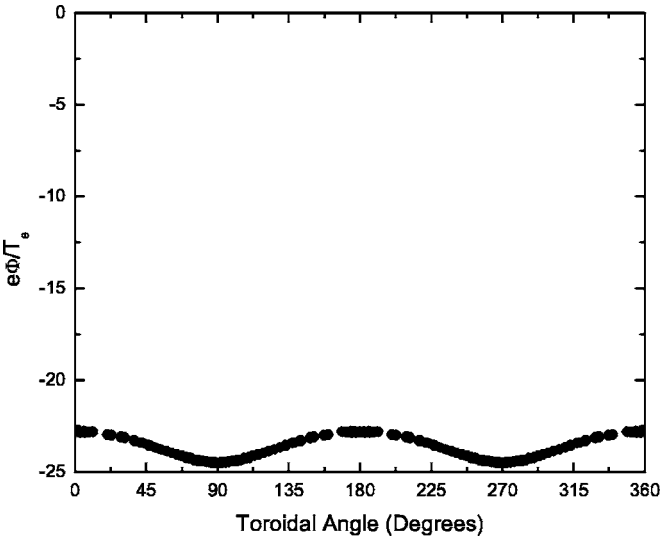

FIG. 4. Axial potential variation, normalized by T_e/e, for a cold electron plasma, $a/\lambda_D \approx 10$.

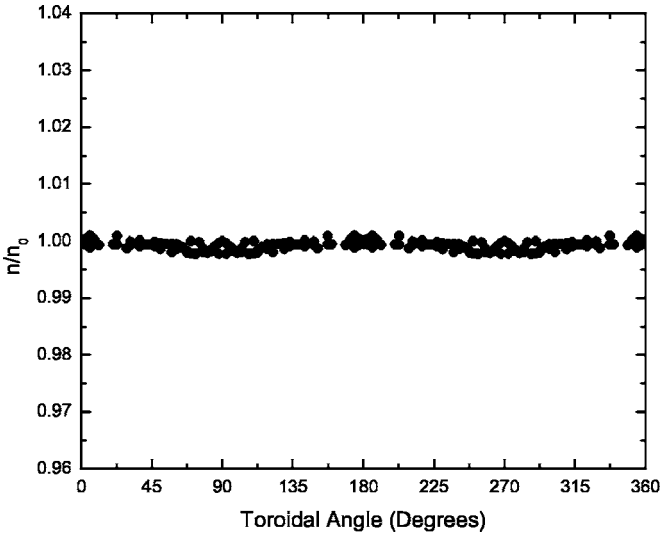

FIG. 5. Normalized axial density variation for a hot electron plasma, $a/\lambda_D \approx 0.1$.

The cross-field potential drop associated with the cylindrical geometry is obtained from Poisson's equation

$$\Delta\Phi_{\perp,\text{cylinder}} = \frac{e n_{\text{axis,cyl.}}}{\epsilon_0} \int_0^a \frac{dq}{q} \int_0^q d\tilde{q}\tilde{q} f(\tilde{q}), \tag{6}$$

and for the slab geometry, with $w_{1/2}$ the half-width

$$\Delta\Phi_{\perp,\text{slab}} = \frac{e n_{\text{axis,slab}}}{\epsilon_0} \int_0^{w_{1/2}} dq \int_0^q d\tilde{q} f(\tilde{q}). \tag{7}$$

Because the potential drop across the field must be constant in the cold limit, we equate Eqs. (6) and (7) to determine the density ratio

$$\frac{n_{\text{axis,slab}}}{n_{\text{axis,cyl.}}} = \frac{\int_0^a \frac{dq}{q} \int_0^q d\tilde{q}\tilde{q} f(\tilde{q})}{\int_0^{w_{1/2}} dq \int_0^q d\tilde{q} f(\tilde{q})}. \tag{8}$$

The ratio of the integral in Eq. (8) is not overly sensitive to the cross-field density profile, $f(q)$. For a standard parabolic profile $[f(q)=1-(q/q_{\text{edge}})^2]$, Eq. (8) yields a ratio of $\frac{9}{20}(a/w_{1/2})^2$, for a flat profile $[f(q)=1]$ the ratio is $\frac{1}{2}(a/w_{1/2})^2$, and for a hollowed parabolic profile $[f(q)=1+(q/q_{\text{edge}})^2]$ the ratio is $\frac{15}{28}(a/w_{1/2})^2$. The variation of the constant in front of $(a/w_{1/2})^2$ is small compared with the uncertainty of our slab approximation, and we can make a good estimate of the variation in density that is dependent only on the geometry of the magnetic field,

$$\frac{n_{\text{axis,slab}}}{n_{\text{axis,cylinder}}} \approx \frac{1}{2}\left(\frac{a}{w_{1/2}}\right)^2. \tag{9}$$

For CNT, the radius of the cylinder-like cross section is 18.0 cm (defined through $A_{cs}=\pi a^2$) and the half-width of the slab-like cross section is 5.6 cm (defined as half of the width of the cross section at the midplane). Inserting these values into Eq. (9) yields a predicted variation of 5.2, in excellent agreement with the computationally obtained variation of 5.3.

Finally, we verify that the potential is roughly constant on axis. Recalling that the (a/λ_D) factor is roughly 10 for this plasma, Eq. (3) suggests that the potential variation on axis should be no more than a few percent of the potential drop across the plasma (perpendicular to the magnetic field). The exact variation can be determined analytically by the Boltzmann relation if the density variation is known,

$$\Phi_1 - \Phi_2 = \frac{T_e}{e} \ln \frac{n_1}{n_2}. \tag{10}$$

This relation predicts an axial variation in potential of $1.65T_e/e$ for the CNT. The computational results shown in Fig. 4 predict a variation of $1.72T_e/e$—the two do not match precisely due to the fact that the Cartesian grid points are not exactly on the magnetic axis. The potential drop across the plasma is just under $25T_e/e$, verifying that the variation in potential along the field is small compared to the potential drop across the plasma.

For the computational results presented above, an equipotential (conducting) boundary has been enforced on the outer magnetic surface.[7] Such a boundary, consisting of copper meshes, has been constructed for CNT, though it has not yet been installed. Additional modeling has been performed for the case in which a conducting boundary is not present, where the boundary conditions are set primarily by the coils, modeled as static distributions of charge on the computational grid. This results in a slightly smaller predicted density variation of 4.4, due to the variation of potential on the boundary.

The large predicted toroidal variation of density in a device such as the CNT provides a robust check of the Debye length of the plasma. For a very hot plasma, $(a/\lambda_D)\approx 0.1$, this variation becomes negligibly small, as shown in Fig. 5. Diagnostics are currently being implemented in the CNT to measure the toroidal density variation.

This material is based upon work supported by the National Science Foundation under Grant No. NSF-PHY-06-13-662.

[1]J. P. Kremer, T. Sunn Pedersen, R. G. Lefrancois, and Q. Marksteiner, Phys. Rev. Lett. **97**, 095003 (2006).
[2]J. de Grassie and J. Malmberg, Phys. Rev. Lett. **39**, 1077 (1977).
[3]T. S. Pedersen and A. H. Boozer, Phys. Rev. Lett. **88**, 205002 (2002).
[4]J. Fajans, Phys. Plasmas **10**, 1209 (2003).
[5]L. Brillouin, Phys. Rev. Lett. **67**, 260 (1945).
[6]T. S. Pedersen, Phys. Plasmas **10**, 334 (2003).
[7]R. G. Lefrancois, T. S. Pedersen, A. H. Boozer, and J. P. Kremer, Phys. Plasmas **12**, 072105 (2005).